Vision Research 77 (2013) 14–20

Contents lists available at SciVerse ScienceDirect

Vision Research

journal homepage: www.elsevier.com/locate/visres

Discrimination of rotated-in-depth curves is facilitated by stereoscopic cues, but curvature is not tuned for stereoscopic rotation-in-depth

Jason Bell [a,*], Jameel Kanji [b], Frederick A.A. Kingdom [b]

[a] Dept. of Psychology, Australian National University, Canberra, ACT 0200, Australia
[b] McGill Vision Research, Dept. of Ophthalmology, McGill University, 687 Pine Av. West, Montreal, QC, Canada H3A 1A1

ARTICLE INFO

Article history:
Received 5 June 2012
Received in revised form 5 October 2012
Available online 27 November 2012

Keywords:
Curvature
Stereo
Viewpoint
Adaptation
Shape
Object

ABSTRACT

Object recognition suffers when objects are rotated-in-depth, as for example with changes to viewing angle. However the loss of recognition can be mitigated by stereoscopic cues, suggesting that object coding is not strictly two-dimensional. Here we consider whether the encoding of rotation-in-depth (RID) of a simple curve is tuned for stereoscopic depth. Experiment 1 first determined that test subjects were sensitive to changes in stereoscopic RID, by showing that stereoscopic cues improved the discrimination of RID when other spatial cues to RID were ineffective. Experiment 2 tested directly whether curvature-sensitive mechanisms were selective for stereoscopic RID. Curvature after-effects were measured for unrotated test curves following adaptation to various RID adaptors. Although strong adaptation tuning for RID angle was found, tuning was identical for stereo and non-stereo adaptors. These findings show that while stereoscopic cues can facilitate three-dimensional curvature discrimination, curvature-sensitive mechanisms are not tuned for stereoscopic RID.

1. Introduction

In normal viewing our visual system must handle a range of image transformations to achieve object recognition. Typical transformations include changes to an object's size, brightness, colour, retinal position and viewpoint. Changes in viewpoint occur every time we, or the object, moves, and numerous studies have reported that the accuracy and speed of object recognition suffers as a result (Bennett & Vuong, 2006; Bulthoff, Edelman, & Tarr, 1995; Burke, 2005; Burke, Taubert, & Higman, 2007; Edelman & Bulthoff, 1992; Lim Lee & Saunders, 2011; Parr, Siebert, & Taubert, 2011). However, stereoscopic cues to the object's 3D (three-dimensional) structure can reduce the costs of viewpoint change (Bell, Dickinson, & Badcock, 2008; Bennett & Vuong, 2006; Bulthoff, Edelman, & Tarr, 1995; Burke, 2005; Burke, Taubert, & Higman, 2007; Lim Lee & Saunders, 2011), supporting the idea that object encoding is not strictly 2D (two-dimensional).

The current study extends that literature by considering the role of stereoscopic cues when encoding viewpoint-rotated shapes. The shape of an object is a powerful cue to its recognition (Attneave, 1954; Bertamini, 2008; Biederman, 1987; Hayworth & Biederman, 2006; Hoffman & Richards, 1984; Hoffman & Singh, 1997; Loffler et al., 2005; Pasupathy & Connor, 2002; Wilkinson, Wilson, & Habak, 1998). Moreover, the curves in an object's outline are more important for recognition than the straight lines. The importance of curves is made explicit in several recent models of shape and/or object perception (Connor, 2004; Pasupathy & Connor, 2002; Poirier & Wilson, 2006, 2010; Yamane et al., 2008).

Previous research, including our own, has examined the selectivity of curvature mechanisms for an orientation change in the 2D plane (Bell, Gheorghiu, & Kingdom, 2009; Timney & Macdonald, 1978). Tight selectivity is reported, with curvature after-effects abolished when a 45° orientation difference between adaptor and test is introduced. This is interpreted as evidence for independent processing of curves with distinct 2D orientations. For higher level objects such as faces, researchers have examined how strongly configural face after-effects (contraction and expansion of internal features) transfer across changes in viewpoint that are consistent with a rotation-in-depth (RID) (Jeffery, Rhodes, & Busey, 2006). Jeffery et al. report that such higher level after-effects persist and are in fact greater than half strength despite a 90° rotational difference between adaptor and test, in other words that they display broad viewpoint tuning. Here we measure the RID selectivity of curvature mechanisms. We aim to compare our findings with analogous studies involving higher level objects such as faces (Jeffery, Rhodes, & Busey, 2006), and to compare RID selectivity in the 3D plane with the reported selectivity for curvature orientation in the 2D plane (Bell, Gheorghiu, & Kingdom, 2009; Timney & Macdonald, 1978).

The primary aim of this communication is to determine whether contour curvature mechanisms are tuned for stereoscopic

* Corresponding author.
E-mail address: Jason.Bell@anu.edu.au (J. Bell).

0042-6989/$ - see front matter Crown Copyright © 2012 Published by Elsevier Ltd. All rights reserved.
http://dx.doi.org/10.1016/j.visres.2012.11.003

RID. In order to test for such tuning, we first establish that humans are *sensitive* to stereoscopic RID in our stimuli. To do this we use a same/different task to measure thresholds for detecting a difference in the RID angle of two curves, with and without stereoscopic cues. Having shown that human observers are able to use stereoscopic cues to discriminate between curves with different RIDs, we go on to ask whether curvature mechanisms are tuned to stereoscopic RID. To address this question we used an adaptation paradigm in which we measure the size of a curvature after-effect, or CAE (Bell, Gheorghiu, & Kingdom, 2009) as a function of the difference in the RID angle between adaptor and test curves. If the CAE is significantly reduced when adaptor and test have different RIDs we conclude that the human visual system is selective for stereoscopic RID.

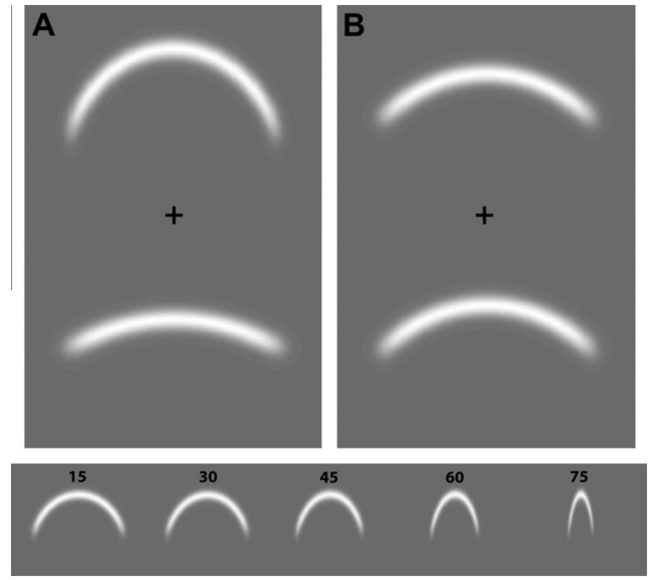

Fig. 1. Curvature after-effect (CAE) and example stimuli. The reader can experience the curvature after-effect by staring at the fixation cross on the left for at least 30 s and then switching their gaze to the fixation cross on the right, where they are likely to perceive the upper curve to be lower in amplitude (more flat) than the lower curve, and *vice versa*. The bottom row (left to right) shows examples of curves with different rotation-in-depth (RID) angles. If the reader free fuses adjacent patterns they may experience the RID stimuli in stereoscopic depth. The RID curves are all identical in their 'sag' i.e. amplitude (0.72°), which is equal to the high amplitude unrotated adaptor in the top left of figure.

2. General methods

2.1. Participants

Nine experienced psychophysical observers participated in the current study. Seven were naïve as to the experimental aims, whilst observers JB and JK were authors. All had normal or corrected-to-normal visual acuity. Each observer's stereo acuity was tested using the Stereo Fly and Stereo Butterfly Test made by Stereo Optical Co., Inc., Chicago. All observers had a stereo acuity better than 40 seconds of arc. Participation was voluntary and unpaid.

2.2. Apparatus and stimuli

Stimuli were created using Matlab version 7.6, and loaded into the frame-store of a Cambridge Research Systems (CRS) ViSaGe video-graphics system. Stimuli were presented on a Sony Trinitron G400 monitor with a screen resolution of 1024 × 768 pixels and a refresh rate of 100 Hz. The luminance of the monitor was calibrated using an Optical OP200-E (Head Model # 265). In all conditions, stimuli were viewed through an 8-mirror stereoscope. The mean luminance of the stimuli as measured through the stereoscope was 34 cd/m^2. The viewing distance through the stereoscope was 55 cm, resulting in each pixel subtending 2′ of visual angle. Prior to testing each observer performed a series of judgments in a control program, whereby they adjusted the horizontal distance between a pair of fixation crosses presented separately to the left and right eye until binocular fusion was achieved. This measurement was then used in the actual experiments.

Example test stimuli are shown in Fig. 1. Each curve represents a half cycle of a sinusoidal shape modulation along the horizontal, producing an inverse U-shaped curve. A contrast smoothing function was applied to each end of the contour to minimise orientation cues at the ends. Each curve was defined by its 'cord' and 'sag', corresponding to the shape-frequency and shape-amplitude of the sinusoidal shape from which the curve was derived. The cross-sectional luminance profile of each contour was a Gaussian with sigma equal to 0.12°.

2.3. Rotation-in-depth

Curves were rotated about their vertical axis, compressing the horizontal dimension of the contour in the fronto-parallel plane. The foreshortening was consistent with a change in horizontal viewing angle (Bell, Dickinson, & Badcock, 2008). In the stereo conditions the curves were rotated-in-depth stereoscopically by presenting a different rotation angle to each eye (+ and − the mean RID angle) (see free fusible examples in Fig. 1: bottom row). In our stereo conditions, all observers reported a vivid impression that the curves were physically rotated-in-depth. The stereoscope was also used in the non-stereo conditions; however in these cases the RID was the same in each eye.

3. Experiments

3.1. Experiment 1: Sensitivity to stereoscopic rotation-in-depth of a simple curve

In this experiment we employed a same/different task to measure thresholds for detecting a difference in RID angle, and compared thresholds with and without stereoscopic cues. We employed a 2IFC (two-interval forced-choice) same/different task (Kingdom & Prins, 2010) rather than conventional 2IFC task so that observers did not have to learn a reference RID angle, nor judge a particular direction of RID angle change. Each trial consisted of two intervals with two curves per interval, i.e. four stimuli per trial. In the reference interval the two curves had the same RID angle (45°) while in the test interval the two curves had different RID angles, and the observer had to choose the interval with the different RID angles. The two curves in each interval were presented 3° above and 3° below a central fixation dot. The method of constant stimuli was employed with 7 RID angle differences. The RID angle difference in the test interval was always symmetrical about 45°, which was also the RID angle of both curves in the reference interval. Each of the seven conditions was presented 20 times, in random order, giving a total of 140 trials per run. A minimum of 4 runs were completed for each observer in each condition, resulting in 560 responses from each observer per condition. The range of RID angle differences was adjusted for each observer in order to obtain a full psychometric function (∼ = 50–100% accuracy). A Logistic function was fit to the data to obtain an estimate of the threshold difference in RID angle corresponding to 75% correct. In Experiment 1a (fixed parameters) the unrotated shape frequency of the curves was set to 0.325c/° and the amplitude of modulation was fixed at 0.4°. In Experiment 1b, both parameters of the curve were randomised independently for each curve on each presentation.

3.2. Results

Fig. 2A (left) shows response data and Logistic fits for three observers in both stereo and non-stereo cue conditions. Each graph plots the proportion of correct responses as a function of the difference in RID angle between the two curves of the test pair. Observers appear to be highly sensitive to a change in RID angle and thresholds for stereo (S) and non-stereo (NS) conditions are near identical [Thresholds: **JK** = 1.68° (S), 1.65° (NS); **JB** = 2.72° (S), 2.32° (NS); **SM** = 2.41° (S), 2.34° (NS)]. An *F*-test of SLOPE and THRESH parameters in Graphpad, Prism (V5) showed that one cannot reject the hypothesis that the data for stereo and non-stereo conditions were best fit by a single Logistic function (**JK** $F_{(2,10)} = 0.04$, $p = 0.95$; **JB** $F_{(2,10)} = 3.21$, $p = 0.08$; **SM** $F_{(2,10)} = 0.04$, $p = 0.96$). A paired samples *t*-test also showed no significant difference between RID angle thresholds in stereo and non-stereo conditions ($t_{(2)} = 1.24$, $p = 0.34$).

Although our non-stereo condition contained zero disparity, the stimuli were viewed binocularly, so it is possible that performance was better than if the stimuli were viewed purely monocularly. To test this possibility a control condition was carried out in which the non-stereo condition of the same/different task was repeated but with a monocular viewing condition included for comparison. In the monocular condition, observers wore an eye patch to prevent binocular viewing and the curves were only presented to the right hand side of the mirror stereoscope, i.e. to the unpatched eye. All other testing procedures were unchanged. Fig. 3 presents the results of this control. Response data and curve fits for the binocular (black points and lines) and monocular (grey points and lines) viewing conditions were identical, consistent with a single curve fit ($F_{(2,10)} = 0.4$, $p = 0.67$). This result shows that on this task, curves viewed binocularly with zero disparity are discriminated in RID no differently than monocularly-viewed examples of the same stimuli. That is, our non-stereo condition involving binocular viewing is entirely representative of non-stereo performance on an RID discrimination task.

As noted by an anonymous reviewer, the two-dimensional projection of an inverse U-shaped curve that has been rotated in depth

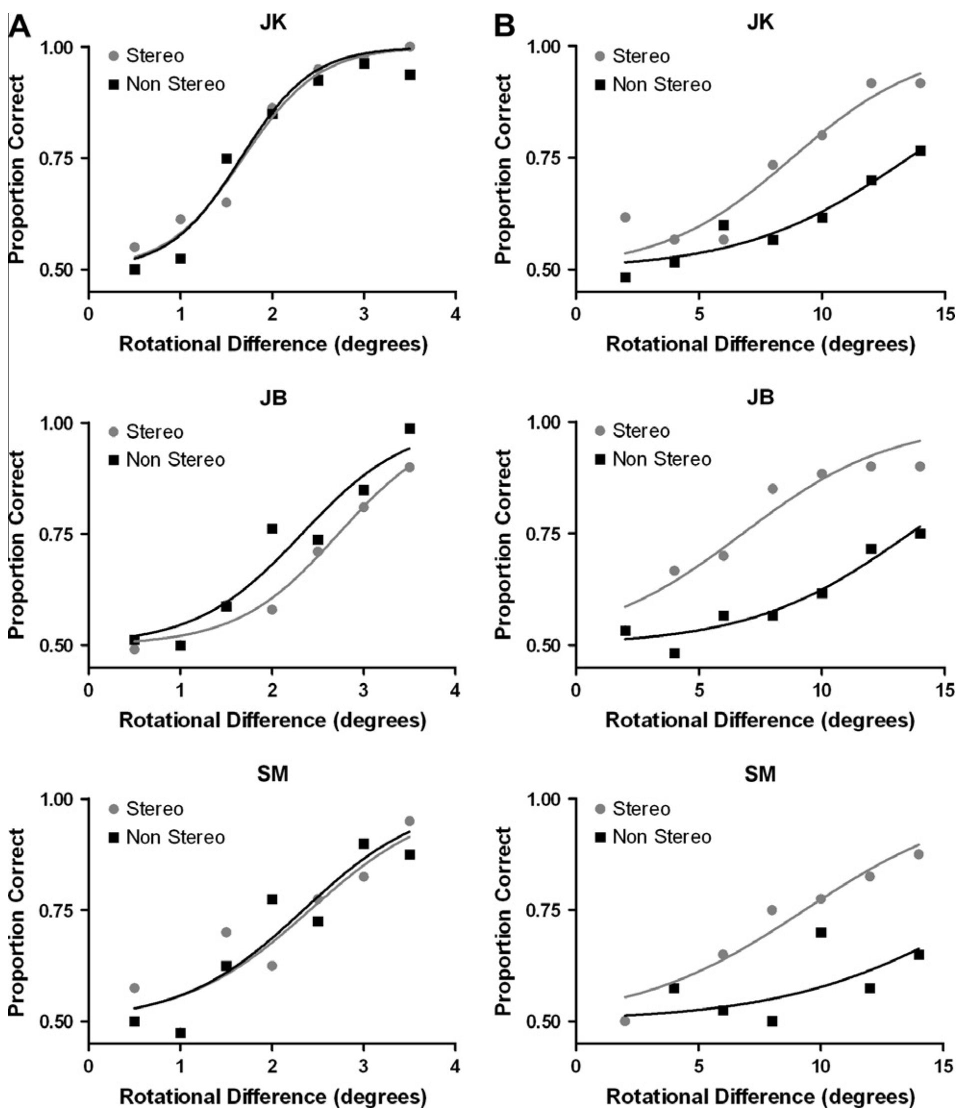

Fig. 2. RID discrimination data. (A) The panels show raw response data and fits for three observers when discriminating between curve pairs with the same or different RID angles. The proportion correct is plotted against the difference in the RID angles of the test pair. Data have been fit by a Logistic function using Graphpad Prism V5. Grey points and lines show data in stereo conditions; black points and lines show non-stereo conditions. There are no discernible differences between the two sets. (B) Same axes and descriptions but now the data is for trials where the size of each curve is randomised on each trial. Note the extended *x* axes, indicating poorer performance overall. Stereo conditions now clearly outperform non-stereo conditions.

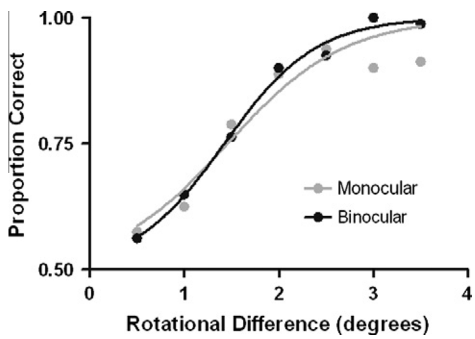

Fig. 3. RID discrimination data for the monocular control condition. The panel plots raw response data and fits for the same/different task employing a zero disparity binocularly viewed stimulus (black points and line) and a strictly monocularly viewed stimulus (grey points and line). There are no discernible differences between the two sets.

is asymmetric, in that the far side of the curve is more compressed than the near side. This asymmetry could be used by the observer to discriminate RID. To test whether observers were sensitive to this asymmetry, three new, naïve observers performed a further control. The three were experienced psychophysical observers but who were unfamiliar with stereo tasks and RID stimuli. Again the same/different task was used. As before, the reference stimuli were 45° RID viewed binocularly with zero disparity. The test stimuli were viewed in the same manner but one curve of the pair was presented at 45° RID while the other was presented at −45° RID (the same RID but opposite in direction). The asymmetries of the two opposite-angled RID stimuli were equal but opposite, i.e. for the 45° RID the left side was more compressed than the right side, whereas for the −45° RID it was the other way around. If the asymmetry in the curves was the basis of discrimination the observers should be able to identify the pair with the opposite RID angles. All three observers were at chance performance on this task (data not shown). Therefore we conclude that the asymmetry in the curves due to RID was not perceptible to the observers and was therefore not a cue in this task.

The question remains however: what feature allowed observers to be so sensitive to a difference in RID in our same/different task? Foreshortening our U-shaped curves caused them to be compressed along their horizontal axes. It is possible that observers based their judgements on the difference in the lengths, or cords of the test pair rather than on perceived RID angle, and if so, it is not surprising that stereo cues did not facilitate performance. To test for the role of the length cue we conducted an additional experiment in which we randomised the size of the curves (both their amplitudes/sags and modulation-frequencies/cords) on each presentation, thus making the two-dimensional projection of the curve an unreliable cue for detecting an RID-angle change. The observer's task was the same as before. Pilot testing revealed that the task was far harder, so the range of RID angle differences was increased.

Fig. 2B (right) shows the results. Although performance is worse in all conditions [compare *x* axis scales for figures in A and B], RID angle difference thresholds are now *significantly lower* in the stereo compared with non-stereo conditions [Thresholds: **JK** = 8.79° (S), 13.54° (NS); **JB** = 6.78° (S), 13.59° (NS); **SM** = 3.47° (S), 16.99° (NS)]. An F test analysis of SLOPE and THRESH parameters showed that, unlike the previous data, two separate Logistic fits to the stereo and non-stereo data were a better fit than a single function (**JK** $F_{(2,10)} = 18.59$, $p = 0.0004$; **JB** $F_{(2,10)} = 43.3$, $p = 0.0001$; **SM** $F_{(2,10)} = 9.54$, $p = 0.0049$). Additionally, a paired samples *t*-test showed a significant difference between RID angle difference thresholds for stereo and non-stereo conditions ($t_{(2)} = 7.4$, $p = 0.01$). The results demonstrate that observers use stereoscopic cues to RID when monocular cues are insufficient.

Given the randomisation of each curve's sag and cord on each trial, it may seem surprising that observers *ever* managed to perform better than chance in the non-stereo conditions. Consider, however, the case of a pair of curves with very different RID angles. Here the introduction of random variation in each curve's size on a given trial is not necessarily greater than the differences between the lengths of the two curves owing to their different RIDs; remember that the greater the RID angle, the greater the horizontal compression of 2D shape. This means that on *some* trials the observer could still use the curve's length to make a correct decision, although clearly not reliably. An inspection of the raw scores in Fig. 2B reveals that no observer ever achieved better than 76% accuracy in the non-stereo condition. This fact does not however challenge our main conclusion, which is that when the *absolute* size of a curve becomes known to the observer, they are highly sensitive to the change in two dimensional profile that accompanies a change in viewing angle (Fig. 2A). In contrast, when randomisation ensures that the absolute size of the curve *cannot* be learnt by the observer, stereo cues are used to discriminate between curves with different RIDs (Fig. 2B).

3.3. Experiment 2: Are curvature encoding mechanisms selective for stereoscopic rotation-in-depth?

Experiment 1 established that subjects are sensitive to stereoscopic RID in our curve stimuli. The question now arises as to whether the mechanisms that encode contour curvature are *selective* for stereoscopic RID, that is tuned to particular stereoscopic RID angles. To investigate this question we measured the size of an established curvature after-effect, or CAE (Bell, Gheorghiu, & Kingdom, 2009) using adapting curves of a variety of RID angles, and un-rotated test curves. We took steps to ensure that the measured after-effects were due to curvature rather than orientation adaptation, in other words that they were not simply the sum of tilt after-effects, or TAEs (Gibson & Radner, 1937), as has been suggested to be the case for some shape after-effects (Blakemore & Over, 1974; Dickinson et al., 2010, 2012). Studies have demonstrated that if adapt and test stimuli differ in parameters such as position, luminance spatial frequency, orientation, luminance polarity, temporal sequence, presentation eye or size, the involvement of TAEs is minimal (Anderson et al., 2007; Bell, Dickinson, & Badcock, 2008; Bell, Gheorghiu, & Kingdom, 2009; Bell & Kingdom, 2009; Burr & Ross, 2008; Gheorghiu & Kingdom, 2007; Gheorghiu et al., 2009; Hancock & Peirce, 2008; Jeffery, Rhodes, & Busey, 2006; Rhodes et al., 2004; Timney & Macdonald, 1978). In our own previous work we have shown that for peripherally viewed stimuli a spatial jitter of one degree of visual angle is sufficient to produce after-effects of curvature (Bell, Gheorghiu, & Kingdom, 2009) and of global shape (Bell & Kingdom, 2009) that are not primarily mediated by local TAEs. Therefore by employing a sufficient amount of spatial jitter we are confident that the after-effects reported below predominantly reflect adaptation of curvature rather than orientation mechanisms.

CAEs were measured for adapting curves with 0°, 15°, 30°, 45°, 60° and 75° rotation (see Fig. 1), and unrotated test curves. In one set of conditions the adapting curves contained stereo cues that enhanced the percept of RID (see Fig. 1 for free-fusible examples). In the other set of conditions the adapting curves had no stereo cues. What are the predictions for this experiment? First, we would expect a reduction in the CAE as a function of the difference in RID angle between adaptor and test even in the non-stereo conditions, because foreshortening a curve decreases its cord length in the fronto-parallel plane and it is known that 2D curvature after-effects are selective for this dimension (Gheorghiu & Kingdom, 2008). Second, if curvature mechanisms are not selective for stereoscopic RID angle then the reduction in the CAE should be identical in stereo and non-stereo conditions. If, on the other hand, curvature mechanisms are selective for stereoscopic RID angle, then the reduction in the CAE should be greater in the stereo compared to non-stereo conditions. Given that stereo cues improve object recognition across viewpoints (Bulthoff, Edelman, & Tarr, 1995; Burke, 2005; Burke, Taubert, & Higman, 2007; Lim Lee & Saunders, 2011), the latter result is predicted.

3.4. Procedure

A staircase procedure was employed to measure the curvature after-effect, or CAE. The procedure was the same as that used by Bell, Gheorghiu, and Kingdom (2009). The initial adaptation period lasted 1 min, during which the spatial location of each set of curves, presented 3° above and 3° below a central fixation dot, was horizontally jittered by a random amount every 500 ms within the range ±0.45°. The unrotated shape frequency of the adapting and test curves was 0.325c/°, giving a cord length of 1.44°, however this varied with RID angle, at least in 2D profile (see Fig. 1). Irrespective of the RID angle, the shape amplitudes of the adapting curves were 0.24° and 0.72°, which are also the sag heights, giving a geometric mean amplitude/sag of 0.4°. Each cycle of the test period began with a 400 ms blank screen, followed by the test pair for 500 ms (signalled by a tone), then a blank screen of 100 ms and finally 2.5 s top-up adaptation. The test stimuli were presented simultaneously 3° above and 3° below the fixation dot (fixation point to the centre of the stimuli). The test pair was always presented in the fronto-parallel plane (0° RID) with no stereo cues. Test stimuli were independently jittered horizontally (±0.5°) on each trial. The observer was instructed to select whether the upper or lower test stimuli appeared to be higher in amplitude i.e. more curved. The amplitude ratio of the test patterns on the first test trial was set to a random number between 0.5 and 1.5 (upper divided by lower) but with the geometric mean amplitude fixed at 0.4°. Following each response (a key press) the computer adjusted the ratio of amplitudes in a direction opposite to that of the response, i.e. towards the point of subjective equality (PSE). For the first 5 trials, the ratio was adjusted by a factor of 1.12, and thereafter by a factor of 1.06. Each run was terminated after 25 trials and the PSE was calculated as the geometric mean ratio of test pattern amplitudes over the last 20 trials, which on average contained 6–10 reversals. Typically, six PSEs were measured for each condition. In half of the sessions, the high amplitude adapting pattern was in the upper visual field whereas in the other half of the sessions the lower amplitude adapting pattern was in the upper visual field. In addition, we measured the PSE in sessions containing no adaptation stimuli; these served as baselines with which to compare the size of the CAE with adaptation. The size of the after-effect calculated for each session was given by the log ratio of test amplitudes (corresponding to the lower and higher adapting amplitudes) at the PSE minus the same PSE value without adaptation. The mean and SE of these values across sessions are the points shown in the graphs.

3.5. Results

CAEs for five observers are shown in Fig. 4. CAEs are plotted as a function of the difference in RID angle between adaptor and test (*x* axis). Grey data points show CAEs in conditions containing stereo cues while black data points show CAEs in non-stereo conditions. The bottom right panel plots the averaged data in each condition. For all observers and for both stereo and non-stereo conditions, CAEs are largest when adaptor and test have the same or similar RID angle. CAEs then systematically decrease in size as the adapting pattern is rotated away from the fronto-parallel plane. This decrease is significant, as shown by a repeated measures 2-way ANOVA ($F_{(4,32)} = 42.95$, $p < .0001$; 0° was not included in this analysis as no 0° stereo CAE was measured). The decline however, is identical for stereo and non-stereo conditions ($F_{(1,8)} = 0.38$, $p = .55$), suggesting that the addition of a stereo cue to RID angle does not affect curvature adaptation. There was no interaction effect ($F_{(4,32)} = 0.14$, $p = .96$).

4. General discussion

Experiment 1 (Fig. 2A) established that observers are sensitive to stereoscopic RID in our curve stimuli. Sensitivity was revealed under conditions in which the size/length of the curve was ineffective as a cue to RID angle. The 'stereo advantage' for viewpoint discrimination of novel shapes reported here is consistent with previous findings from studies involving discrimination between unfamiliar faces, or between abstract objects (Bennett & Vuong, 2006; Bulthoff, Edelman, & Tarr, 1995; Burke, 2005; Burke, Taubert, & Higman, 2007; Edelman & Bulthoff, 1992). It would appear that stereoscopic cues are useful for discriminating between different views of an object, particularly if there is uncertainty with regard to object properties such as curve length, or the rotation of a bent paperclip. It must be remembered though that the stereo advantage evidenced here is for discrimination of a change in RID angle, rather than discrimination between different objects. In the object viewpoint literature observers are typically assessed on their ability and/or speed to discriminate between objects across different viewpoints, whereas our observers were required to discriminate between (simulated) viewpoints of a single shape.

Experiment 2 investigated whether curvature-sensitive mechanisms are selective for stereoscopic RID. We found that curvature adaptation is strongly tuned for the RID relationship between adaptor and test (Fig. 4): CAEs measured with fronto-parallel test curves systematically decreased as the adapting curves were rotated in depth away from the fronto-parallel plane. However the tuning function was identical in stereo and non-stereo conditions, implying that curvature-sensitive mechanisms are not tuned for stereoscopic RID. This result is consistent with a previous finding that curvature-sensitive mechanisms, while predominantly binocular, are not selective for the plane of stereoscopic depth (Gheorghiu et al., 2009). Finally, our finding that stereo and non-stereo adaptors produce identical curvature after-effects is itself further evidence that our after-effects are not simply due to local TAEs. Using a non-stereoscopic line as a test, Wolfe and Held (1982) report that a stereoscopically viewed adapting line produces a smaller TAE than does a non-stereoscopic adaptor. The implication of which is that if local TAEs were underpinning our findings, then the after-effects reported in our Fig. 4 should have been reduced in the stereo cue added conditions. Clearly this is not the case.

How does the tuning of curvature mechanisms to RID compare to the tuning to orientation of a curve as it is rotated within the 2D plane, as evidenced by Timney and Macdonald (1978) and Bell, Gheorghiu, and Kingdom (2009). In Bell et al.'s study, CAEs were completely abolished when the adaptor was rotated just 45° clockwise relative to the test, whereas in the present study measurable CAEs were obtained even for a 75° RID adaptor-test difference. The likely reason for these differences is that a given curvature mechanism will respond to a larger proportion of the available range of orientations in the RID versus 2D-orientation cases, on the grounds that the cross-correlation between adaptor and test will on average be greater in the former condition.

Face after-effects are also tuned for viewpoint (Fang & He, 2005; Jeffery, Rhodes, & Busey, 2006), though a direct comparison with

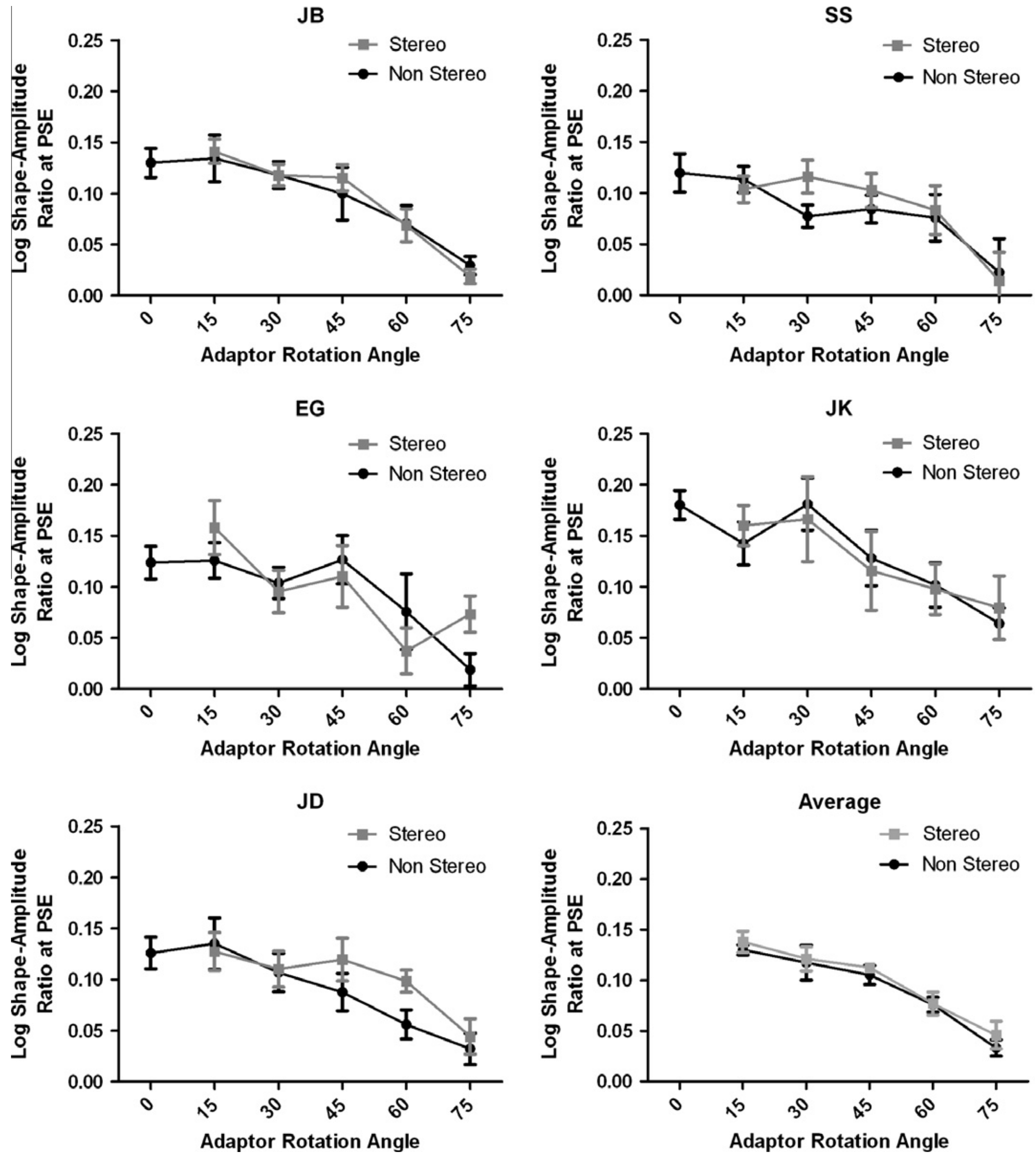

Fig. 4. Curvature after-effect (CAE) size plotted as a function of adaptor RID angle. Data for five observers is shown: averaged data is in the boxed plot, bottom right. In all figures the size of the CAE is plotted on the *y* axis and the RID angle of the adapting pair on the *x* axis. The test was always at 0° RID with no stereo cues added. Grey points again show data for conditions in which stereo cues to RID angle were included; black points show non-stereo conditions. Data in both conditions are near identical. Error bars show ±1 std. error.

the present study is somewhat problematic. For instance in Jeffery et al.'s study of configural face after-effects (contracted or expanded features), adapt and test viewpoint differences were 45°, much larger than the 15° differences employed here. Also, Jeffery et al. did not test stereoscopic cues to face viewpoint. However there are in principle similarities between our and Jeffery et al.'s adaptation procedures for 2D stimuli; namely, both studies measured the size of an appearance based after-effect as a function of the difference in viewing angle between adaptor and test. Going onto compare the respective 2D data, an inspection of Jeffery et al.'s non-stereo data reveals that for a 90° viewpoint difference between adaptor and test, the configural face after-effect was still approximately 50%; whereas in our study CAEs declined by almost 80% for a smaller 75° viewpoint difference (Fig. 4).

There is evidence for viewpoint-specific face and object processing mechanisms in the Lateral Occipital Cortex, LOC and Fusiform Face Area, FFA (Grill-Spector et al., 1999; Kourtzi & Grill-Spector, 2005), but it remains to be seen whether such mechanisms are selective for stereoscopic disparity, as the 'stereo advantage' for viewpoint rotated objects would imply. While there is evidence that neurons in monkey IT cortex utilise stereoscopic cues to encode 3D object shape and viewpoint (Janssen, Vogels, & Orban, 2000a, 2000b; Uka et al., 2000; Yamane et al., 2008), there are no physiological studies to our knowledge that have demonstrated that the parts-of-shapes, such as curves, are processed by neurons sensitive to either the plane of stereoscopic depth or to stereoscopic RID. Curves are believed to be processed in intermediate form processing regions, such as area V4, where the 2D orientation and position properties of curvature selective cells have been well documented in monkey V4 (Bushnell et al., 2011; Muller, Wilke, & Leopold, 2009; Pasupathy & Connor, 1999, 2001; Yau et al., 2010) and to a lesser extent in human V4 (Gallant, Shoup, & Mazer, 2000; Wilkinson et al., 2000). Our findings extend the literature on curvature processing by investigating the selectivity of curvature encoding mechanisms for stereoscopic RID.

In summary, we have demonstrated (1) that human observers are highly sensitive to a change in the RID angle of a curve, (2) that stereoscopic cues do not facilitate RID discrimination unless the 2D profile of the curve cannot be used as a point of reference, and (3) that curvature-sensitive mechanisms are not tuned to stereoscopic RID. Therefore, consistent with the assumptions of recent neurophysiological models of shape and object coding (Pasupathy & Connor, 2002; Yamane et al., 2008), we conclude that the representation of RID of a curve is 2D.

Acknowledgments

This research was supported by the Australian Research Council (ARC) Discovery Project (Grant # DP110101511) given to J.B. and the Natural Sciences and Engineering Research Council (NSERC) of Canada, (Grant # OGP01217130) given to F.K.

References

Anderson, N. D., Habak, C., Wilkinson, F., & Wilson, H. R. (2007). Evaluating shape after-effects with radial frequency patterns. *Vision Research, 47*(3), 298–308.

Attneave, F. (1954). Some informational aspects of visual perception. *Psychological Review, 61*(3), 183–193.

Bell, J., Dickinson, J. E., & Badcock, D. R. (2008). Radial frequency adaptation suggests polar-based coding of local shape cues. *Vision Research, 48*(21), 2293–2301.

Bell, J., Gheorghiu, E., & Kingdom, F. A. A. (2009). Orientation tuning of curvature adaptation reveals both curvature-polarity-selective and non-selective mechanisms. *Journal of Vision, 9*(12), 1–11.

Bell, J., & Kingdom, F. A. A. (2009). Global contour shapes are coded differently from their local components. *Vision Research, 49*(13), 1702–1710.

Bennett, D. J., & Vuong, Q. C. (2006). A stereo advantage in generalizing over changes in viewpoint on object recognition tasks. *Perception and Psychophysics, 68*(7), 1082–1093.

Bertamini, M. (2008). Detection of convexity and concavity in context. *Journal of Experimental Psychology – Human Perception and Performance, 34*(4), 775–789.

Biederman, I. (1987). Recognition-by-components: A theory of human image understanding. *Psychological Review, 94*(2), 115–147.

Blakemore, C., & Over, R. (1974). Curvature detectors in human vision? *Perception, 3*(1), 3–7.

Bulthoff, H. H., Edelman, S. Y., & Tarr, M. J. (1995). How are three-dimensional objects represented in the brain? *Cerebral Cortex, 5*(3), 247–260.

Burke, D. (2005). Combining disparate views of objects: Viewpoint costs are reduced by stereopsis. *Visual Cognition, 12*(5), 705–719.

Burke, D., Taubert, J., & Higman, T. (2007). Are face representations viewpoint dependent? A stereo advantage for generalising across different views of faces. *Vision Research, 47*(16), 2164–2169.

Burr, D., & Ross, J. (2008). A visual sense of number. *Current Biology, 18*(6), 425–428.

Bushnell, B. N., Harding, P. J., Kosai, Y., Bair, W., & Pasupathy, A. (2011). Equiluminance cells in visual cortical area V4. *The Journal of Neuroscience, 31*(35), 12398–12412.

Connor, C. E. (2004). Shape dimensions and object primitives. In L. M. Chalupa & J. S. Werner (Eds.), *The visual neurosciences* (pp. 1080–1089). London: MIT Press.

Dickinson, J. E., Almeida, R. A., Bell, J., & Badcock, D. R. (2010). Global shape aftereffects have a local substrate: A tilt aftereffect field (Research Support, Non-U.S. Gov't). *Journal of Vision, 10*(13), 5.

Dickinson, J. E., Mighall, H. K., Almeida, R. A., Bell, J., & Badcock, D. R. (2012). Rapidly acquired shape and face aftereffects are retinotopic and local in origin. *Vision Research, 65*, 1–11.

Edelman, S., & Bulthoff, H. H. (1992). Orientation dependence in the recognition of familiar and novel views of three-dimensional objects. *Vision Research, 32*(12), 2385–2400.

Fang, F., & He, S. (2005). Viewer-centered object representation in the human visual system revealed by viewpoint aftereffects. *Neuron, 45*(5), 793–800.

Gallant, J. L., Shoup, R. E., & Mazer, J. A. (2000). A human extrastriate area functionally homologous to macaque V4. *Neuron, 27*(2), 227–235.

Gheorghiu, E., & Kingdom, F. A. (2007). The spatial feature underlying the shape-frequency and shape-amplitude after-effects. *Vision Research, 47*(6), 834–844.

Gheorghiu, E., & Kingdom, F. A. (2008). Spatial properties of curvature-encoding mechanisms revealed through the shape-frequency and shape-amplitude after-effects. *Vision Research, 48*(9), 1107–1124.

Gheorghiu, E., Kingdom, F. A., Thai, M. T., & Sampasivam, L. (2009). Binocular properties of curvature-encoding mechanisms revealed through two shape after-effects. *Vision Research, 49*(14), 1765–1774.

Gibson, J. J., & Radner, M. (1937). Adaptation, after-effect and contrast in the perception of tilted lines. *Journal of Experimental Psychology, 20*, 453–467.

Grill-Spector, K., Kushnir, T., Edelman, S., Avidan, G., Itzchak, Y., & Malach, R. (1999). Differential processing of objects under various viewing conditions in the human lateral occipital complex. *Neuron, 24*(1), 187–203.

Hancock, S., & Peirce, J. W. (2008). Selective mechanisms for simple contours revealed by compound adaptation. *Journal of Vision, 8*(7), 1–10.

Hayworth, K. J., & Biederman, I. (2006). Neural evidence for intermediate representations in object recognition. *Vision Research, 46*(23), 4024–4031.

Hoffman, D. D., & Richards, W. A. (1984). Parts of recognition. *Cognition, 18*(1–3), 65–96.

Hoffman, D. D., & Singh, M. (1997). Salience of visual parts. *Cognition, 63*(1), 29–78.

Janssen, P., Vogels, R., & Orban, G. A. (2000a). Selectivity for 3D shape that reveals distinct areas within macaque inferior temporal cortex. *Science, 288*(5473), 2054–2056.

Janssen, P., Vogels, R., & Orban, G. A. (2000b). Three-dimensional shape coding in inferior temporal cortex. *Neuron, 27*(2), 385–397.

Jeffery, L., Rhodes, G., & Busey, T. (2006). View-specific coding of face shape. *Psychological Science, 17*(6), 501–505.

Kingdom, F. A. A., & Prins, N. (2010). *Psychophysics: A practical introduction*. London: Academic Press (an imprint of Elsevier).

Kourtzi, Z., & Grill-Spector, K. (2005). FMRI adaptation: A tool for studying visual representations in the primate brain. In C. W. Clifford & G. Rhodes (Eds.), *Fitting the mind to the world: Adaptation and aftereffects in high-level vision* (pp. 173–188). Oxford: Oxford University Press.

Lim Lee, Y., & Saunders, J. A. (2011). Stereo improves 3D shape discrimination even when rich monocular shape cues are available. *Journal of Vision, 11*(9).

Loffler, G., Yourganov, G., Wilkinson, F., & Wilson, H. R. (2005). FMRI evidence for the neural representation of faces. *Nature Neuroscience, 8*(10), 1386–1390.

Muller, K. M., Wilke, M., & Leopold, D. A. (2009). Visual adaptation to convexity in macaque area V4. *Neuroscience, 161*(2), 655–662.

Parr, L. A., Siebert, E., & Taubert, J. (2011). Effect of familiarity and viewpoint on face recognition in chimpanzees. *Perception, 40*(7), 863–872.

Pasupathy, A., & Connor, C. E. (1999). Responses to contour features in macaque area V4. *Journal of Neurophysiology, 82*(5), 2490–2502.

Pasupathy, A., & Connor, C. E. (2001). Shape representation in area V4: Position-specific tuning for boundary conformation. *Journal of Neurophysiology, 86*(5), 2505–2519.

Pasupathy, A., & Connor, C. E. (2002). Population coding of shape in area V4. *Nature Neuroscience, 5*(12), 1332–1338.

Poirier, F. J. A. M., & Wilson, H. R. (2006). A biologically plausible model of human radial frequency perception. *Vision Research, 46*(15), 2443–2455.

Poirier, F. J. A. M., & Wilson, H. R. (2010). A biologically plausible model of human shape symmetry perception. *Journal of Vision, 10*(1), 1–16.

Rhodes, G., Jeffery, L., Watson, T. L., Jaquet, E., Winkler, C., & Clifford, C. W. (2004). Orientation-contingent face aftereffects and implications for face-coding mechanisms. *Current Biology: CB, 14*(23), 2119–2123.

Timney, B. N., & Macdonald, C. (1978). Are curves detected by 'curvature detectors'? *Perception, 7*(1), 51–64.

Uka, T., Tanaka, H., Yoshiyama, K., Kato, M., & Fujita, I. (2000). Disparity selectivity of neurons in monkey inferior temporal cortex. *Journal of Neurophysiology, 84*(1), 120–132.

Wilkinson, F., James, T. W., Wilson, H. R., Gati, J. S., Menon, R. S., & Goodale, M. A. (2000). An fMRI study of the selective activation of human extrastriate form vision areas by radial and concentric gratings. *Current Biology, 10*(22), 1455–1458.

Wilkinson, F., Wilson, H. R., & Habak, C. (1998). Detection and recognition of radial frequency patterns. *Vision Research, 38*(22), 3555–3568.

Wolfe, J. M., & Held, R. (1982). Binocular adaptation that cannot be measured monocularly. *Perception, 11*(3), 287–295.

Yamane, Y., Carlson, E. T., Bowman, K. C., Wang, Z., & Connor, C. E. (2008). A neural code for three-dimensional object shape in macaque inferotemporal cortex. *Nature Neuroscience, 11*(11), 1352–1360.

Yau, J., Pasupathy, A., Brincat, S., & Connor, C. (2010). Dynamic synthesis of curvature in area V4. *Journal of Vision, 10*(7), 911.